Supporting Information

Non-specific binding of RNA to PARP1 and PARP2 does not lead to catalytic activation

Meagan Y. Nakamoto[1‡], Johannes Rudolph[1‡], Deborah S. Wuttke[1], Karolin Luger[1,2,*]

[1]Department of Biochemistry, University of Colorado Boulder, Boulder, CO 80309, USA

[2]Howard Hughes Medical Institute, University of Colorado Boulder, Boulder, CO 80309, USA

[‡]These authors contributed equally to this work.

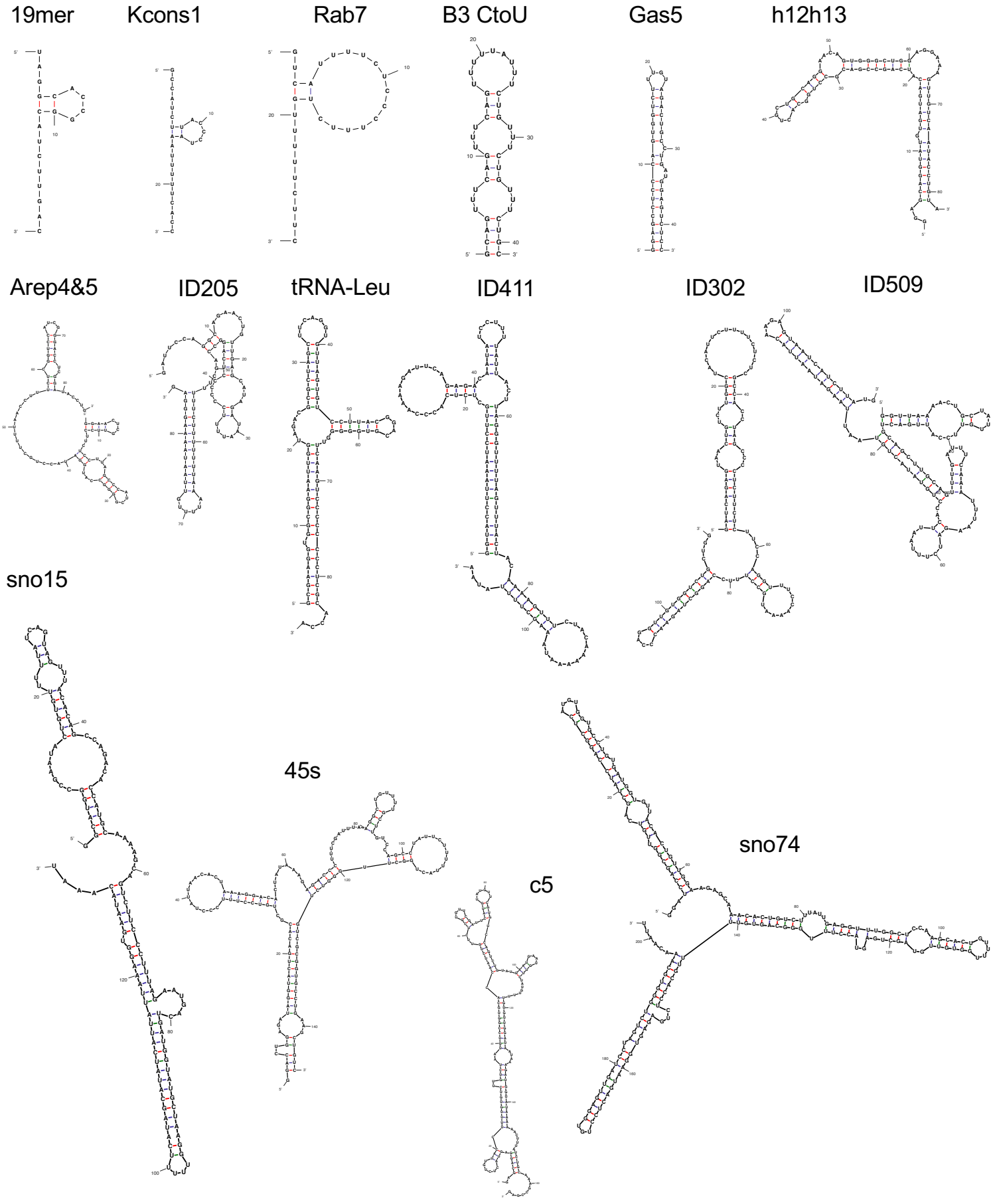

Figure S1: Predicted lowest energy secondary structure for the RNAs used in this study as determined by mfold (Nucleic Acids Res. **31**, 3406-3415, 2003). Kcons3 and env8 RNAs are not shown as no stable folds were predicted for these sequences.

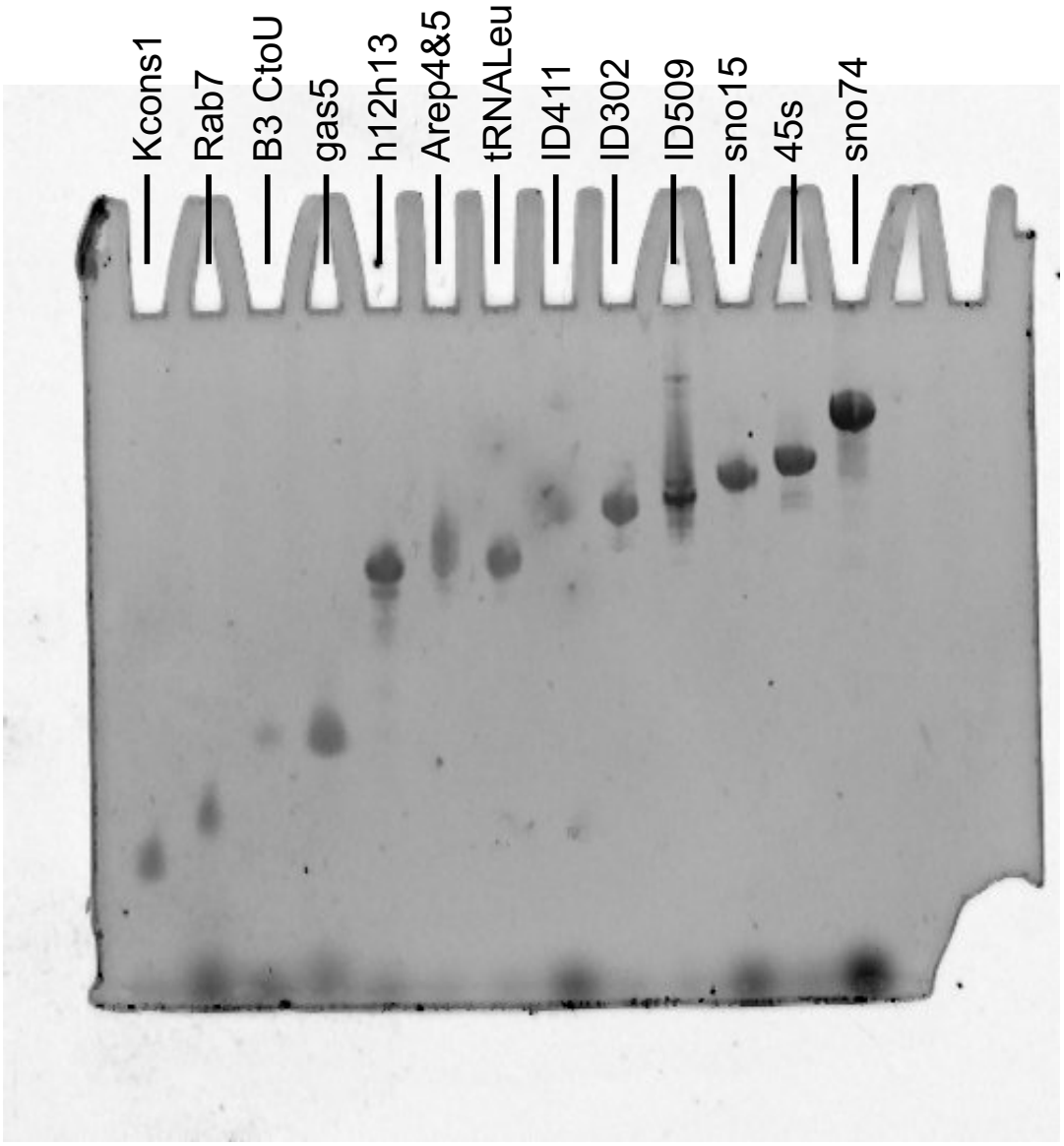

Figure S2: Representative denaturing gel (10% acrylamide, 8 M urea) demonstrating purity and size of transcribed RNAs. The gel was stained for 1 h with 1x Sybr Green II (ThermoFisher) in TBE and visualized on a Typhoon imager (GE Healthcare) using the ethidium bromide settings (980 PMT, 200 µm resolution).

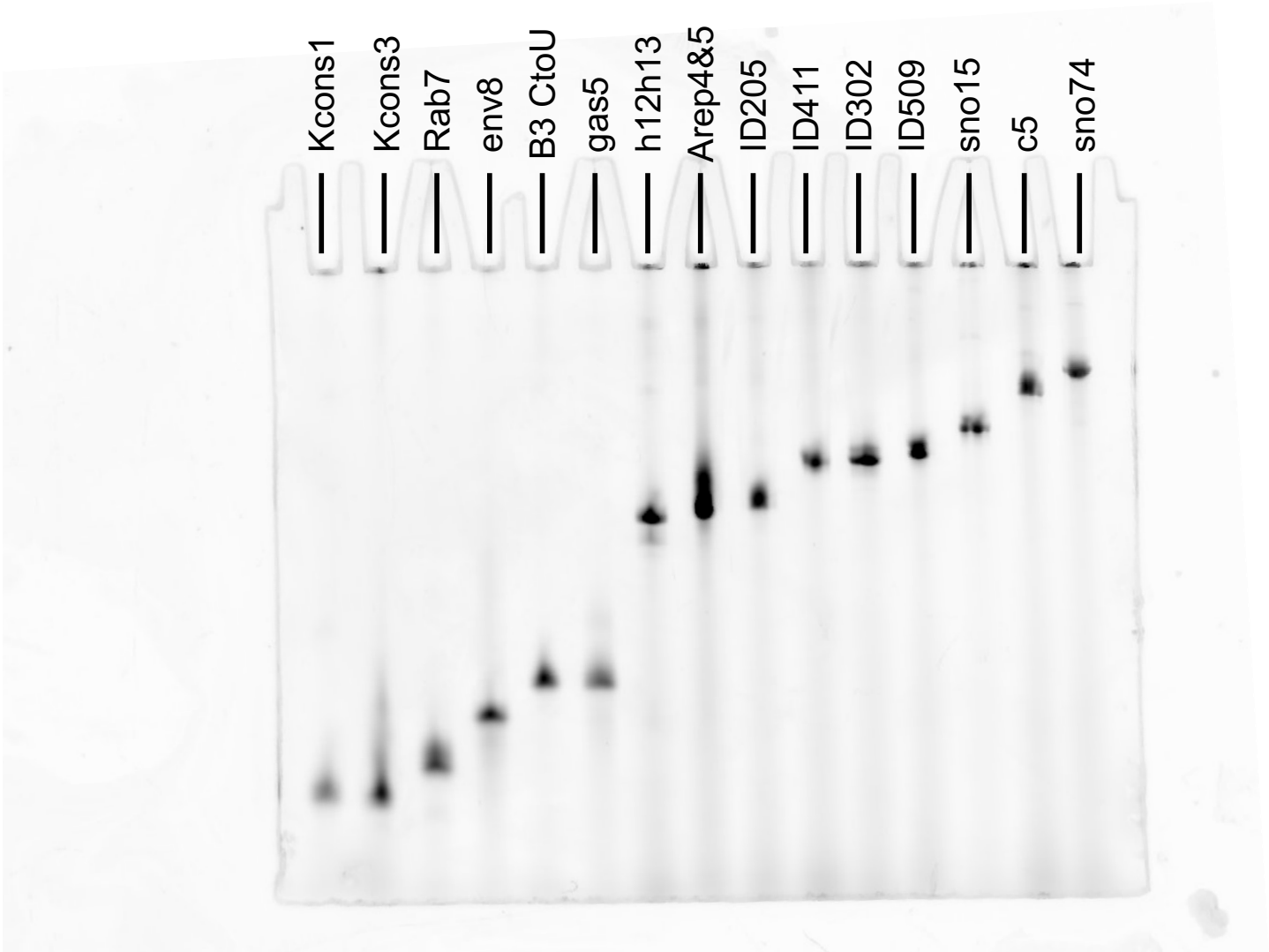

Figure S3: Representative denaturing gel (10% acrylamide, 8 M urea) demonstrating purity and size of FTSC-end-labeled RNAs. The gel was visualized on a Typhoon imager (GE Healthcare) using the Cy2 filter (400 PMT, 200 µm resolution).

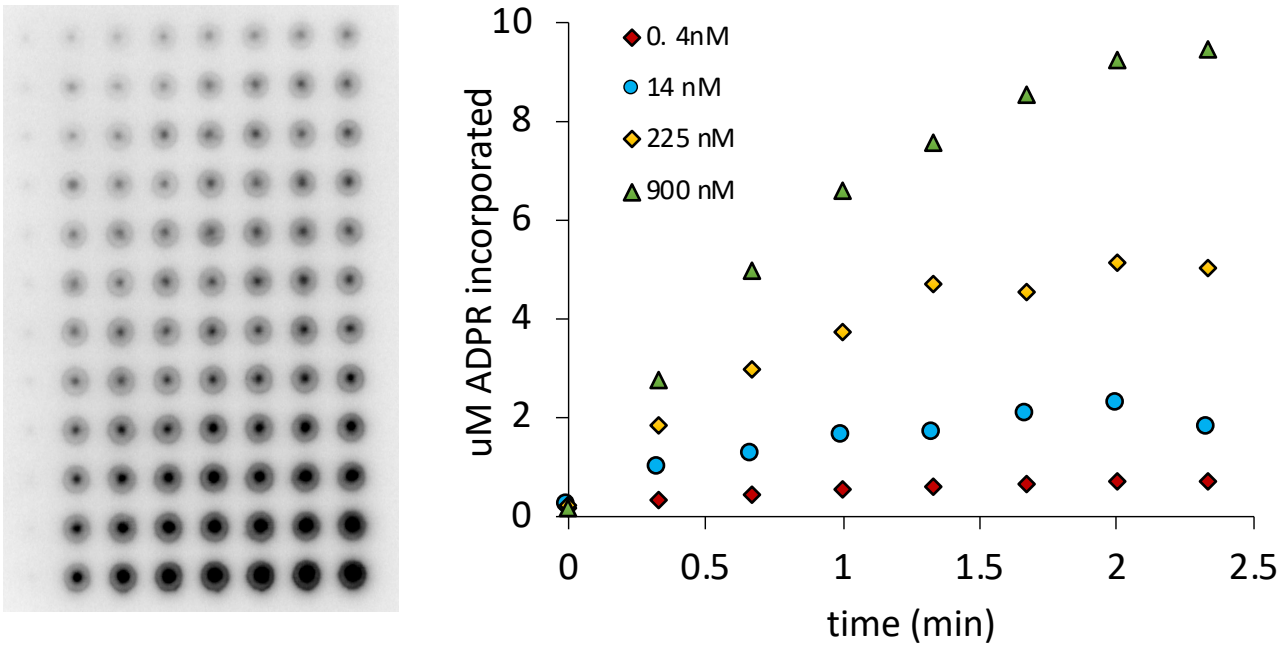

Figure S4: Demonstrating the linearity of PARylation by PARP1. Left: Increasing concentrations of p18mer DNA (0.4 – 900 nM, rows) were incubated with PARP1 (30 nM) and ^{32}P-NAD (40 μM) for varying lengths of time (0 – 160 s, columns). PARylated protein was captured and quantitated in a filtration assay as described in the Methods. Right: Representative time-courses from the raw images shown on the left demonstrating that PARylation is only linear for a short reaction time (<1.5 min).

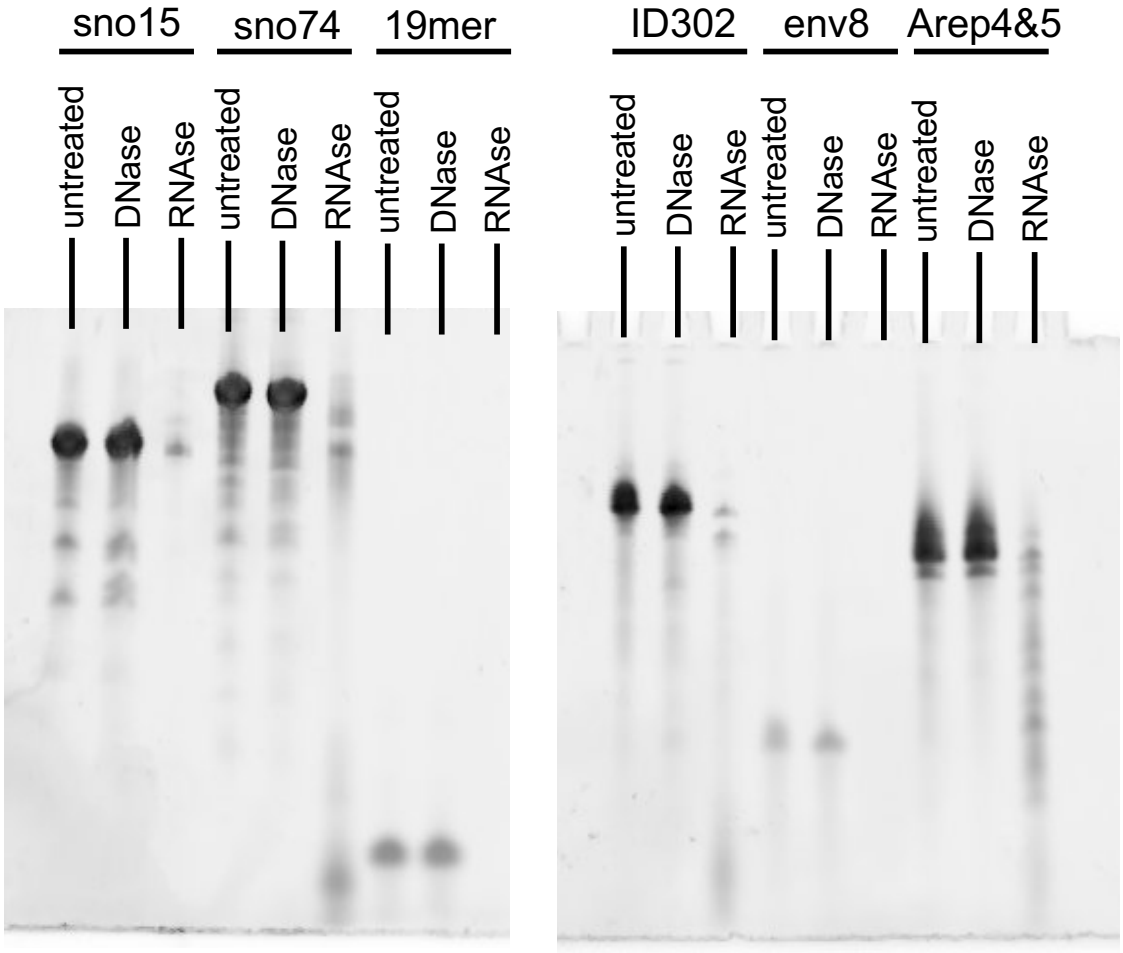

Figure S5: Representative denaturing gels (10% acrylamide, 8 M urea) demonstrating effectiveness of RNase treatment of RNAs. The gels were stained for 45 min with 1x Sybr Green II (ThermoFisher) and 30 min with Sybr Gold (ThermoFisher) in TBE and visualized on a Typhoon imager (GE Healthcare) using the Cy2 filter (400 PMT, 200 µm resolution).

RNA	nt	sequence
19mer	19	UAGGCACCGGCAUCUUGAC
Kcons1	25	GCCAUCUUACCCUAAAUUUUUCACC
Kcons3	25	GCCAUCCCACCCUACCCUUUUCACC
Rab7	31	GUCAUUUUCUCCCUUUCUGUUUUUCUUC
env8	35	AUACAACAUACAACAUACAACAUACAACAUACAAC
B3 CtoU	41	GCAGUUUCAGUUUCAGUUUUUAUUUCUGUUUCUGUUUCUGC
gas5	43	GGAGCCUCCCAGUGGUCUUUGUAGACUGCCUGAUGGAGUCUCC
h12h13	82	GGAGCAGGUAUGUGAUGACAUCAGCCGACGCCUGGCACUGCUGCAGGAACAGUGGGCUGGAGGAAAGUUGUCAAUACCUGUA
Arep4&5	85	GGAACUCGUUCCUUCUCCUUAGCCCAUCGGGGCCAUGGAUACCUGCUUUUAACCUUUCUCGGUCCAUCGGGACCUCGGAUACCUG
ID205	86	GAUUCCAGGCAGAACUGUUGAGCAUAGAUAAUUUUCCCCCCUCAGGCCAGCUUUUUCUUUUUUUAAAUUUUGUUAAUAAAAGGGAG
tRNALeu	87	GCGAAGGUGGCGGAAUUGGUAGACGCGCUAGCUUCAGGUGUUAGUGUCCUUACGGACGUGGGGGUUCAAGUCCCCCCCCUCGCACCA
ID411	109	GGUACCUUAAAUCCUUGCUCUCACCCAAAAGAUUCAGAGACAAUAUCCUUUUAUUACUUAGGGUUUUAGUUUACUACAAAAGUUUCUACAAAAAAUAAAGCUUUUAUAA
ID302	111	GAUCAGAGUAACUGUCUUGGCUACAUUCUUUUCUCUCGCCACCUAGCCCCUCUUCUCUUCCAGGUUUCCAAAAUGCCUUUCCAGGCUAGAACCCAGGUUGUGGUCUGCUGG
ID509	114	GGUUAAAACUGCUAUUGUUCCAUUGACUGCAGCUUGCAGUUUGAUUUCAAAUUUAAGAUCUUUAAUUCACCUGUAUACUGUAAUUAAGAUAAUUACAAGAGUAAUCAUCUUAUG
sno15	134	GGCAUGGCCGAAUACUGUGUUUUUAUCAGUAGUUUACACAGCCAGACACCAUGCAAAAGCAGUCUUCCCUUUAGAAUGACUGAUGGUAUGCUAAGGUUUUUCAUAGCAUAUCAUUAUUAAAGGUGAAUACAAAU
45s	146	GGACCUGGAGAUAGGUACUGACACGCUGUCCUUUCCCUAUUAACACUAAAGGACACUAUAAAGAGACCCUUUCGAUUUAAGGCUGUUUUGCUUGUCCAGCCUAUUCUUUUUACUGGCUUGGGUCUGUCGCGGUGCCUGAAGCUGUC
c5	166	GAGCAGGAGUACUCUGUUACCUUUUGUGUCUUGUCUAAUGUCCGGUGCACCAAUCUGUUCUCGUGUUCGAUUCAUGUAUGUUCGUGUCCAGUCUGUAUGAAUGAAUGUUCUAUGUUUUGUGUUGGAUAAUAAAGAUGGUAUAAAAAACUUUAUCUGCAAAGCCGAG
sno74	202	GGAUCCAGCGGUUGUCAGCUAUCCAGGCUCAUGUGGUGCCUGUGAUGGUGUUACACUGUUGGAAGAGCAAACACUGUCUUUAUUGAGGUUUGGCUCCAAGCACUGUUUUGGUGUUGUAGCUGAGUACCUUUGGGCAGUGUUUUGCACCUCUGAGAGUGGAAUGACUCCUGUGGAGUUGAUCCUAGUCUGGGUGCAAACAAUU

Table S1: List of RNAs including sequence used in this study.

DNA template preparation for in vitro transcription

The sequences for all the RNA constructs used in this study are listed in Supplementary Table 1. cDNAs of all RNA constructs (except 19mer) were ordered either as gBlocks (for long transcripts >41 nt) or as standard DNA oligonucleotides (for short transcripts <42 nt) from IDT, incorporating the T7 promoter on the 5'-end. If ordered as a gBlock, primers flanking the cDNA but containing the EcoRI and BamHI cut sites on the 5′ and 3′ ends respectively were used to PCR amplify the gBlock for restriction enzyme cloning into a pUC19 vector. Ligated plasmids were verified using Sanger sequencing (Quintara Biosciences) prior to DNA transcription template generation via PCR. For these long transcripts, standard PCR using the cloned vector was used to generate dsDNA *in vitro* transcription templates for run-off transcription. For short transcripts, sense and antisense DNA oligos are annealed at 2 μM (5 min 95°C, slow cool to 25°C in 10 mM Tris (pH 7.5), 1 mM EDTA, 50 mM NaCl) to generate dsDNA *in vitro* transcription templates for run-off transcription.

RNA transcription

RNAs were prepared by performing *in vitro* transcription on dsDNA templates with in-house prepared T7 polymerase (Batey Lab, CU Boulder)[1]. Transcription reactions were gel purified on 5-12% acrylamide, 8 M urea, 1X TBE slab gels[2]. Purified RNA concentrations and quality were assessed by the A_{260} and the A_{260}/A_{280} ratio. RNA transcription products were qualitatively assessed for purity using denaturing gel electrophoresis (Supplementary Figure 2). Concentrations were calculated using the extinction coefficient provided for each RNA sequence by the Scripps extinction coefficient calculator (adapted and utilized in: http://www.fechem.uzh.ch/MT/links/ext.html). Typically, a 200 μL transcription reaction yielded 2.5 nmol of RNA and had a A_{260}/A_{280} ratio of 2.0.

Fluorescent End-labeling of RNA

Purified RNA was 3′-end labeled with fluorescein-5-thiosemicarbazide (FTSC, Sigma) to perform fluorescence binding assays using a published protocol[3,4]. Importantly, this method only labels RNA, not DNA, because of the requirement of an adjacent 2'-OH. Fluorescein labeled products were qualitatively assessed for purity and labeling efficiency via denaturing gel electrophoresis (Supplementary Figure 3). The Cy2 filter on the Typhoon imager (GE Healthcare) was used to visualize the attached label. RNA concentrations were determined post-labeling by A_{260} measurements. FTSC-labeled RNA was stored in dark amber tubes at -20°C.

Treatment of RNA with RNase and DNase

1.4 units of DNaseI (NEB) or 0.15 μg/mL of in-house RNase A were added to 10 μL reactions containing 5 – 10 μM of purified RNA in 1x DNaseI buffer (10 mM Tris pH 7.6, 2.5 mM $MgCl_2$, 0.5 mM $CaCl_2$) and allowed to react for 45-55 min at 37°C. The reactions were aliquoted and stored at -20°C. Thawed aliquots were used to perform PARP activity assays and analysis by native polyacrylamide gel analysis followed by SYBR Green II staining.

Expression and Purification of PARP1
Wild-type human PARP1 and PARP2 were expressed and purified from *E. coli* as previously described[5] with the minor modification that both PARP1 and PARP2 were eluted from the nickel-NTA column using a gradient from 20 – 400 mM imidazole.

Binding of RNA to PARP1/2 as detected by fluorescence polarization
PARP1 was serially diluted (1.5:1) from 2 μM in binding buffer (50 mM Tris-HCl, pH 8.0, 50 mM NaCl, 1 mM $MgCl_2$, 0.1 mM EDTA, 0.01% IGEPAL) in rows of a 96-well plate (Costar3898), and 10 μL of each dilution were transferred to rows of a 384-well plate (Costar9017) with the last four columns containing only buffer as a control. Fluorescently labeled RNAs were diluted to 10 nM in binding buffer, heated to 95°C for 45 seconds, and then chilled on ice for 5+ min. Individual diluted RNAs were then added to rows of the 384-well plate. The fluorescent polarization (FP) signal was measured using a BMG Labtech Clariostar instrument with excitation at 482 nm, a 504 nm dichroic cut-off filter, and 530 nm emission. Binding constants (K_d) were determined by fitting the observed fluorescence polarization signal (FP_{obs})

$$FP_{obs} = FP_{min} + \left\{(FP_{max} - FP_{min}) * ((K_d + P + R) - \sqrt{(K_d + P + R)^2 - 4 * P * R))}\right\} / 2R$$

where FP_{max} is the highest observed FP signal at saturation, FP_{min} is the lowest FP measured in the control wells in the absence of protein (fixed at control value), P is the concentration of protein (0.06 – 1000 nM), and R is the concentration of the probe RNA (5 nM). Control experiments using RNase treated RNA showed no change in FP signal, indicating that FITC dye alone does not bind to either PARP1 or PARP2.

PARP1/2 activity as detected by incorporation of ^{32}P-ADPR
PARP1 (30 nM) or PARP2 (60 nM) were pre-incubated with varying concentrations of DNA (0.01 – 200 nM final) or fixed concentrations of RNA (1 μM) in assay buffer (50 mM Tris-HCl, pH 8.0, 50 mM NaCl, 1 mM $MgCl_2$, 0.1 mM EDTA, 0.5 mg/mL bovine serum albumin (Ambion)) in 96-well plates (Costar3898). Following addition of ^{32}P-NAD^+ (40 μM, 1.8 x 10^6 cpm/well, PerkinElmer) to yield a final volume of 25 μL, reactions were quenched at 30 s by addition of 50 μL of 30% trichloracetic acid (TCA). Samples (50 μL of total) were then loaded onto a Whatman Mini-Fold Spot-Blot apparatus containing a Whatman GF/C glass microfiber filter. Each well was washed three times with 10% TCA (100 μL). After removal of the filter from the apparatus, the filter was gently incubated in 10% TCA (20 – 40 mL) for three more washes. After drying, the filter was exposed to a phosphoimager screen overnight (GE Healthcare) and imaged using a Typhoon 9500 (GE Healthcare). Spot intensities were quantitated using ImageQuant. Activation constants for DNA (K_{act}) were determined by fitting the observed incorporation of radioactivity (cpm_{obs}) to

$$cpm_{obs} = cpm_{min} + \frac{(cpm_{max} - cpm_{min})}{(1 + (\frac{[DNA]}{K_{act}})}$$

where cpm_{min} is derived from control samples containing no DNA activator, cpm_{max} is the highest observed incorporation, and [DNA] is the concentration of DNA. The percentage of activation by RNA ($\%_{act}$) was determined by fitting to

$$\%_{act} = \frac{(cpm_{\max\,(RNA)} - cpm_{\min\,(control)})}{(cpm_{\max\,(DNA)} - cpm_{\min\,(control)}}$$

where cpm_{min} is derived from control samples containing no DNA activator, $cpm_{max(DNA)}$ is the highest observed incorporation at 200 nM DNA (saturating), and $cpm_{max(RNA)}$ is the highest observed incorporation at 1 μM RNA. Control experiments using assay buffer as above with 12.5 mM $MgCl_2$ to compare with other published assay conditions showed K_{act} for DNA to increase 20 – 50-fold for both PARP1 and PARP2 compared to 1 mM $MgCl_2$, and did not lead to RNA-mediated activation of either PARP1 or PARP2 (data not shown).

References

(1) Milligan, J. F.; Groebe, D. R.; Witherell, G. W.; Uhlenbeck, O. C. Oligoribonucleotide Synthesis Using T7 RNA Polymerase and Synthetic DNA Templates. *Nucleic Acids Res.* **1987**, *15* (21), 8783–8798. https://doi.org/10.1093/nar/15.21.8783.

(2) Nilsen, T. W. Gel Purification of RNA. *Cold Spring Harb. Protoc.* **2013**, *2013* (2), pdb.prot072942. https://doi.org/10.1101/pdb.prot072942.

(3) Zearfoss, N. R.; Ryder, S. P. End-Labeling Oligonucleotides with Chemical Tags After Synthesis. In *Recombinant and In Vitro RNA Synthesis: Methods and Protocols*; Conn, G. L., Ed.; Methods in Molecular Biology; Humana Press: Totowa, NJ, 2012; pp 181–193. https://doi.org/10.1007/978-1-62703-113-4_14.

(4) Parsonnet, N. V.; Lammer, N. C.; Holmes, Z. E.; Batey, R. T.; Wuttke, D. S. The Glucocorticoid Receptor DNA-Binding Domain Recognizes RNA Hairpin Structures with High Affinity. *Nucleic Acids Res.* **2019**. https://doi.org/10.1093/nar/gkz486.

(5) Langelier, M.-F., Planck, J. L., Servent, K. M., and Pascal, J. M. (2011) Purification of Human PARP-1 and PARP-1 Domains from Escherichia coli for Structural and Biochemical Analysis, in *Methods in Molecular Biology*, pp 209–226.